

An angular power spectrum analysis of the DRAO 1.4 GHz polarization survey: implications for CMB observations

L. La Porta^{1,*}, C. Burigana², W. Reich¹, and P. Reich¹

¹ Max-Planck-Institut für Radioastronomie, Auf dem Hügel, 69, D-53121 Bonn, Germany

² INAF-IASF Bologna, via P. Gobetti, 101, I-40129 Bologna, Italy

Submitted May 3, 2006; in revised form May 26, 2006.

ABSTRACT

Aims. The aim of the present analysis is to improve the knowledge of the statistical properties of the Galactic diffuse synchrotron emission, which constrains sensitive CMB anisotropy measurements.

Methods. We have analysed the new DRAO 1.4 GHz polarization survey together with the Stockert 1.4 GHz total intensity survey and derived the angular power spectra (APSs) of the total intensity, the polarized emission, and their cross-correlation for the entire surveys and for three low-intensity regions.

Results. The APSs of the diffuse synchrotron emission are modelled by power laws. For the E and B modes, a slope of $\alpha \sim [-3.0, -2.5]$ for the multipole range $\sim [30, 300]$ is found. By the extrapolation of these results to 70 GHz, we can estimate the Galactic synchrotron contamination of CMB anisotropies, and we find results that are compatible with the ones coming from WMAP 3-yr data. In the low-intensity regions, the cosmological primordial B mode peak at $\ell \sim 100$ should be clearly observable for a tensor-to-scalar ratio $T/S \gtrsim 0.5$ and a synchrotron temperature spectral index $\beta \sim -3$. Its detection is also possible for $T/S \gtrsim 0.005$ and $\beta \sim -3$, in case a separation of the foreground from the CMB signal could be achieved with an accuracy of $\sim 5 - 10\%$. For the TE mode, a mask excluding $|b_{gal}| \leq 5^\circ$ (for $\beta \sim -3.0$) or $|b_{gal}| \leq 20^\circ$ (for $\beta \sim -2.8$) from the surveys is sufficient to render the foreground contamination negligible, thus confirming the ability of WMAP to have a clear view of the temperature-polarization correlation peak and antipeak series.

Key words. Polarization – Galaxy: general – Cosmology: cosmic microwave background – Methods: data analysis.

1. Introduction

The polarized Galactic diffuse synchrotron radiation is expected to be the major foreground at $\nu \lesssim 70$ GHz on intermediate and large angular scales ($\theta \gtrsim 30'$) at medium and high Galactic latitudes. At about 1 GHz, the synchrotron emission is the most important radiative mechanism out of the Galactic plane. Consequently, radio frequencies are the natural range for studying it, though it might be affected by Faraday rotation and depolarization. Before the DRAO survey became available, the Leiden polarization surveys (Brouw & Spoelstra 1976) provided a sky coverage, allowing to estimate the Galactic synchrotron APS on intermediate and large scales (La Porta & Burigana 2006). However, these surveys have sparse sampling, low sensitivity, and a good signal-

to-noise ratio only for the brightest regions in the sky. A new linear polarization survey of the northern celestial hemisphere at 1.42 GHz with an angular resolution $\theta_{HPBW} \simeq 36'$ has recently been completed using the DRAO 26 m telescope (Wolleben et al. 2006). The survey has a spacing, θ_s , of $15'$ in right ascension and from $0^\circ:25$ to $2^\circ:5$ in declination, which requires interpolation to construct equidistant cylindrical (ECP) maps with $\theta_{pixel} = 15'$ (Wolleben 2005). The final map has an rms-noise of about 12 mK, which is unique so far in terms of sensitivity. The polarized intensity map appears cold and patchy at high Galactic latitudes, except for the “North Polar Spur” (NPS), extending far out of the plane at about $\ell_{gal} \sim 30^\circ$. We used the polarization data in combination with the Stockert total intensity map at 1.42 GHz (Reich 1982; Reich & Reich 1986), having the same angular resolution, similar sensitivity, and $\theta_s \simeq 15'$, to investigate

Send offprint requests to: C. Burigana

* Member of the International Max Planck Research School (IMPRS) for Radio and Infrared Astronomy at the Universities of Bonn and Cologne.

¹ The NPS has been extensively studied (see Egger & Aschenbach (1995) and references therein) and is interpreted as the shock front of an evolved local supernova remnant.

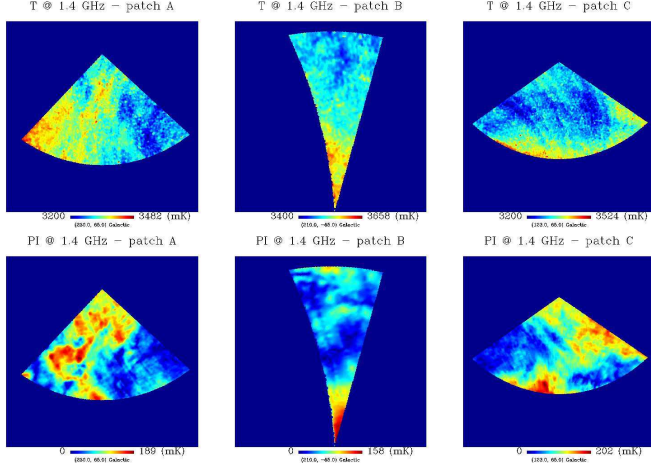


Fig. 1. Gnomonic projection of the cold patches representative of the diffuse Galactic synchrotron emission at 1.4 GHz (total intensity – top panels; polarization – bottom panels).

the statistical properties of the Galactic diffuse synchrotron emission. The major purpose of the analysis is the comparison of the foreground fluctuation properties with those of the CMB anisotropy field, as drawn in standard cosmologies. Therefore, we described the anisotropy field statistical properties in terms of its angular power spectrum (APS)² (see Peebles 1993; Kamionkowski et al. 1997; Zaldarriaga 2001) and adopted HEALPix³ (Górski et al. 2005) as the tessellation scheme for the sphere. A detailed description of the algorithm to convert the original ECP maps into HEALPix maps was given by La Porta et al. (2005).

2. Selected areas and data analysis

We selected three areas with low polarized intensities (see Fig. 1), which are identified by the following Galactic coordinates: Patch A - $180^\circ \leq \ell_{gal} \leq 276^\circ$, $b_{gal} \geq 45^\circ$; Patch B - $193^\circ \leq \ell_{gal} \leq 228^\circ$, $b_{gal} \leq -45^\circ$; Patch C - $65^\circ \leq \ell_{gal} \leq 180^\circ$, $b_{gal} \geq 45^\circ$. Being interested in the diffuse Galactic synchrotron emission at 1.4 GHz, we subtracted discrete sources (DSs) from the total intensity map (very few sources are visible in polarization out of the plane). We performed a 2-dimensional Gaussian fitting using the NOD2-software library (Haslam 1974), which also allowed us to estimate the diffuse background. We are confident that at $|b_{gal}| \gtrsim 45^\circ$ DSs with peak flux densities exceeding ~ 1 Jy have been removed that way (see Burigana et al. 2006 for a map of the subtracted DSs).

We then derived the APSs of the fluctuation fields (i.e., after subtraction of the mean value from the maps) for the three selected areas and the whole survey coverage using the HEALPix facility `anafast`. Figure 2 shows the APSs obtained for the selected areas in both temperature and polarization.

In all cases, the polarization APSs are rather similar⁴. This fact might indicate that depolarization due to differential

² The angular scale θ and the angular power spectrum multipole ℓ are related by $\ell \sim 180^\circ/\theta[^\circ]$.

³ <http://healpix.jpl.nasa.gov/>

⁴ In particular, $C_\ell^E \simeq C_\ell^B$. We then introduce the quantity $C_\ell^{E:B} = 0.5 \cdot (C_\ell^E + C_\ell^B)$, which will be used in the following best-fit analysis. On

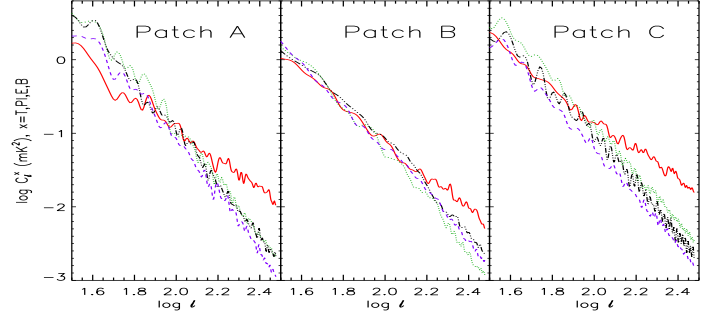


Fig. 2. APSs of the selected cold regions (solid lines $\rightarrow C_\ell^{TI}$; dashes $\rightarrow C_\ell^{PI}$; dots $\rightarrow C_\ell^E$; three dots-dashes $\rightarrow C_\ell^B$).

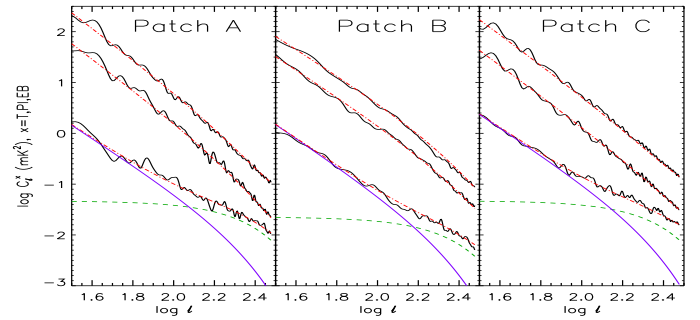


Fig. 3. APSs of the selected cold regions and corresponding best-fit curves (dot-dashed lines). From the bottom: C_ℓ^{TI} , $20 \cdot C_\ell^{PI}$ and $50 \cdot C_\ell^{E:B}$. In the case of C_ℓ^{TI} , $C_\ell^{synch} e^{-(\sigma_b \ell)^2}$ and $c_\ell^{src} e^{-(\sigma_b \ell)^2}$ are also displayed.

Coverage		Best-fit parameters		
		$\log_{10} k$ (mK ²)	α	c^{src} (mK ²)
A	C_ℓ^{TI}	4.067 ^{-1.027} _{+0.682}	-2.60 ^{+0.60} _{-0.40}	0.046 ^{-0.027} _{+0.016}
	C_ℓ^{PI}	5.000 ^{-0.420} _{+0.200}	-3.07 ^{+0.22} _{-0.11}	0.002 ^{-0.002} _{+0.002}
	$C_\ell^{E:B}$	5.2550 ^{-0.305} _{+0.324}	-3.05 ^{+0.15} _{-0.17}	0.003 ^{-0.003} _{+0.001}
B	C_ℓ^{TI}	4.239 ^{-0.611} _{+0.016}	-2.71 ^{+0.34} _{-0.01}	0.023 ^{-0.013} _{+0.008}
	C_ℓ^{PI}	4.146 ^{-0.105} _{+0.553}	-2.62 ^{+0.07} _{-0.35}	0.003 ^{-0.003} _{+0.005}
	$C_\ell^{E:B}$	4.041 ^{-0.112} _{+0.405}	-2.55 ^{+0.06} _{-0.30}	0.003 ^{-0.003} _{+0.005}
C	C_ℓ^{TI}	4.339 ^{-0.297} _{+0.284}	-2.64 ^{+0.03} _{-0.01}	0.047 ^{-0.030} _{+0.013}
	C_ℓ^{PI}	4.748 ^{-0.350} _{+0.650}	-2.94 ^{+0.20} _{-0.36}	0.004 ^{-0.004} _{+0.004}
	$C_\ell^{E:B}$	4.954 ^{-0.301} _{+0.444}	-2.94 ^{+0.20} _{-0.26}	0.005 ^{-0.005} _{+0.009}

Table 1. Least-square best-fit parameters describing the APSs of the selected patches in the range $30 \leq \ell \leq 300$. The errors are given so that the upper (resp. lower) values correspond to the best-fit parameters set with the flattest (resp. steepest) slope.

Faraday rotation should not be relevant in such sky regions at the investigated angular scales. In fact, rotation measure (RM) maps (Johnston-Hollitt et al. 2004; Dineen & Coles 2005) obtained interpolating RM data of extragalactic sources show very low values in correspondence to such areas. However, the degree of polarization is on average a few percent, well below the maximum theoretical value of $\sim 75\%$ (Ginzburg & Syrovatskii 1965). The reason for the low fractional polarization is not clear. One possibility is that de-

the contrary, the E and B modes of the primordial CMB anisotropies differ largely as they are induced by different mechanisms (e.g., Seljak & Zaldarriaga 1997; Kosowsky 1999).

polarization other than differential depolarization is present (e.g., Sokoloff et al. 1998).

The maps show the Galactic synchrotron emission and non-subtracted DSs convolved with the telescope beam and contaminated by noise. We then fitted the APSs of both total intensity and polarization (namely C_ℓ^{TI} , C_ℓ^{PI} , and $C_\ell^{E:B}$) by modelling them as $C_\ell = (C_\ell^{synch} + c^{src}) \cdot W_\ell + c^{WN}$. We exploited the power law approximation $C_\ell^{synch} = \kappa \cdot \ell^\alpha$ and assumed a symmetric Gaussian beam, i.e., a window function $W_\ell = e^{-(\sigma_b \ell)^2}$, where $\sigma_b = \theta_{HPBW}(\text{rad}) / \sqrt{8 \ln 2}$. The contribution of non-subtracted DSs has been simply modelled with a constant term according to the formalism of Poisson fluctuations from extragalactic point sources (Toffolatti et al. 1998), expected to represent the largest fraction of the non-subtracted DSs. From extragalactic source counts at 1.4 GHz (Prandoni et al. 2001) we estimate $c^{src} \simeq 0.09 \text{ mK}^2$ for C_ℓ^{TI} (adding or subtracting quoted 1σ errors to the best-fit number counts we (conservatively) get $c^{src} \simeq [0.05 - 0.3] \text{ mK}^2$). A guess of the noise contribution is given by $C_\ell^{WN} \sim 4\pi \cdot \sigma_{pix} / N_{pix}$, where N_{pix} is the number of pixels in the HEALPix map and $\sigma_{pix} = \sigma_{pix,HEALPix} \sim N^{-1/2} \cdot \sigma_{pix,ECP}$, N being the number of the ECP pixels corresponding to each HEALPix pixel at a given latitude (for the total intensity maps of the selected areas, $\sigma_{pix,HEALPix} \sim 13 \text{ mK}$ corresponding to $c^{WN} \sim 0.003 \text{ mK}^2$). The best-fit results for all patches are listed in Table 1 and shown in Fig. 3. For temperature, the parameter range for the Galactic synchrotron emission APS is $\alpha \sim [-2.71, -2.60]$ for the slope and $\log_{10} \kappa \sim [4.067, 4.339]$ (κ in mK^2) for the amplitude. The DS contribution is in the range $c^{src} \sim [0.023, 0.047] \text{ mK}^2$, which is consistent with the above source counts estimate, within the errors⁵. For polarization, the derived slopes are generally steeper, varying in the interval $\alpha \sim [-3.02, -2.62]$ for C_ℓ^{PI} and $\alpha \sim [-3.05, -2.55]$ for $C_\ell^{E:B}$. The DS contribution is on average much lower than in temperature, since it is compatible with zero⁶.

3. Discussion: implications for CMB observations

We have extrapolated the recovered APS of the E and B modes to 70 GHz and compared it with the APS of the CMB polarization

anisotropy⁷ for a Λ CDM model including scalar and tensor perturbations compatible with the recent WMAP 3-yr results⁸ (Spergel et al. 2006). The frequency range between 60 GHz and 80 GHz seems the less contaminated by Galactic synchrotron and dust foregrounds in both temperature (Bennett et al. 2003) and polarization (Page et al. 2006) at angular scales $\gtrsim 1^\circ$. The accurate measure of the E mode is of particular relevance for breaking the existing degeneracy in cosmological parameter estimation, when only temperature anisotropy data are available (e.g., Bond et al. 1995, Efstathiou & Bond 1999). The detection of the primordial B mode is of fundamental importance for testing the existence of a stochastic cosmological background of gravitational waves (e.g., Knox & Turner 1994). The results of our comparison have been displayed in Fig. 4 for two choices of the temperature spectral index ($\beta = -2.8, -3$). The APS extrapolated from the entire DRAO survey is also shown. It exceeds the CMB E mode even at the peak at $\ell \sim 100$ for $\beta = -2.8$. For $\beta = -3$, the two APSs are almost comparable. Figure 4 also shows the APS extrapolated from the DRAO survey excluding the region $|b_{gal}| \leq 20^\circ$ and adopting $\beta = -3$ ⁹. Such a sky mask reduces the Galactic APS below the CMB E mode for $\ell \gtrsim 50$.

In this case, the CMB B mode peak at $\ell \sim 100$ is comparable to (or exceeds) the synchrotron signal for tensor-to-scalar ratios $T/S \gtrsim 0.5$. For the three patches and $T/S \gtrsim 0.5$, the cosmological B mode peak at $\ell \sim 100$ is comparable to (or exceeds) the Galactic synchrotron signal extrapolated with $\beta \simeq -2.8$, while it is larger by a factor $\gtrsim 2$ (in terms of $\sqrt{C_\ell}$) for $\beta \simeq -3$. Furthermore, a separation of the Galactic synchrotron polarized signal from the CMB one with a $\sim 5 - 10\%$ accuracy (in terms of $\sqrt{C_\ell}$) would allow to detect the CMB B mode peak at $\ell \sim 100$ even for $T/S \sim 0.005$ if $\beta \simeq -3$. Similar results for the detection of the B mode peak at $\ell \sim 100$ have been inferred from 1.4 GHz polarization observations of a small region with exceptionally low Galactic foreground contamination (Carretti et al. 2006), though at $\ell \sim \text{few} \times 100$ the CMB B mode is expected to be dominated by the B mode generated by lensing (Zaldarriaga & Seljak 1998). Finally, we note that for a sky coverage comparable with those of the considered patches ($\sim 3\%$), the cosmic and sampling variance does not significantly limit the accuracy of the CMB mode recovery at ℓ larger than some tens.

The CMB TE correlation constrains the reionization history from the power at low multipoles and the nature of primordial fluctuations from the series of peaks and antipeaks (e.g., Kogut 2003; Page et al. 2006). In Fig. 5 we compare the TE mode APS of the Galactic emission extrapolated to 70 GHz with the CMB one. The APS of the whole DRAO survey indicates a significant Galactic contamination at $\ell \lesssim \text{few} \times 10$, even for $\beta \simeq -3$. The use of suitable Galactic masks (e.g., excluding regions at $|b_{gal}| \leq 5^\circ$ for $\beta \sim -3$ or $|b_{gal}| \leq 20^\circ$ for $\beta \sim -2.8$)

⁵ The bulk of the factor ~ 2 of discrepancy between the value of c^{src} recovered by our fit and that predicted from best-fit number counts can in fact be produced by the survey sky sampling (θ_s) of $15'$. For example, considering a lower limit corresponding to $\simeq 15' / \sqrt{2}$ (instead of 0) in the integral over ψ in Eq. (2) of Toffolatti et al. (1998), c^{src} decreases by a factor $\simeq 1.53$.

⁶ The best-fit results may suggest a polarization degree (obtained considering the contribution of the subtracted DSs, $\sim 0.05 - 0.2 \text{ mK}^2$, to the temperature APS also) considerably higher than $\sim 2\%$, the value found for NVSS extragalactic (mainly steep spectrum) sources (Mesa et al. 2002; Tucci et al. 2004). It may imply a presence (or a combination) of spurious instrumental polarization at small scales, of a significant contribution from highly polarized Galactic sources (Manchester et al. 1998) non-subtracted in the maps, or of a flattening of the diffuse synchrotron polarized emission APS at $\ell \gtrsim 200 - 250$ in higher resolution data on smaller sky areas (Baccigalupi et al. 2001; Carretti et al. 2006).

⁷ We used the CMBFAST code (version 4.5.1) for the computation of the CMB APS (<http://www.cmbfast.org/>).

⁸ <http://lambda.gsfc.nasa.gov/>

⁹ This APS is consistent with the WMAP foreground polarization APS at 63 GHz (see Fig. 17 in Page et al. 2006), thus supporting an effective 1.4 – 70 GHz polarization spectral index $\beta \simeq -3$ far out of the Galactic plane.

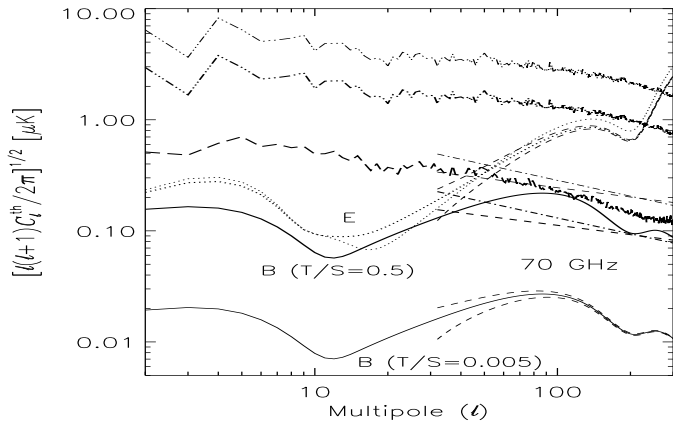


Fig. 4. Comparison between the E and B modes of the CMB anisotropy at 70 GHz and of the Galactic polarized synchrotron foreground. Dotted and solid lines: CMB E and B mode for two different tensor-to-scalar ratios (thin line $T/S = 0.005$, thick line $T/S = 0.5$). Dashed lines: uncertainty associated with the cosmic and sampling variance for a sky coverage of $\sim 3\%$ and a binning of 10% in ℓ . Three dots-dashes: average of the E and B modes extrapolated from the whole DRACO survey for spectral indices $\beta = -2.8$ and -3 , respectively. The anafast results have been divided by the window function to correct for beam smoothing. Thick long dashed line: the same as above, but with a mask at $|b_{gal}| \leq 20$ for $\beta = -3$. Dashed (dot-dashed) power law: best-fit result corresponding to Patch B (resp. C), rescaled in frequency as above. The results are here in terms of thermodynamic temperature.

greatly reduces the Galactic foreground contamination even at low multipoles. For the three cold patches, the Galactic TE mode is negligible compared to the CMB one, independently of the adopted β . The TE mode antipeak at $\ell \sim 150$ turns out to be very weakly affected by Galactic synchrotron contamination in all cases.

Acknowledgements. We warmly thank G. De Zotti and L. Toffolatti for useful discussions. We are grateful to R. Wielebinski for a careful reading of the original manuscript. We warmly thank the anonymous referee for constructive comments. Some of the results in this paper have been derived using HEALPix (Górski et al. 2005). The use of the CMBFAST code (version 4.5.1) is acknowledged. L.L.P. was supported for this research through a stipend from the International Max Planck Research School (IMPRS) for Radio and Infrared Astronomy at the Universities of Bonn and Cologne.

References

- Baccigalupi, C., Burigana, C., Perrotta, F. et al. 2001, *A&A*, 372, 8
 Bennett, C. L., Hill, R. S., Hinshaw, G. et al. 2003, *ApJS*, 148, 97
 Bond, J. R., Davis, R. L., & Steinhardt, P. J. 1995, *ApL&C*, 32, 53
 Brouw, W. N., & Spoelstra, T. A. T. 1976, *A&AS*, 26, 129
 Burigana, C., La Porta, L., Reich, P., & Reich, W. 2006, *AN*, 327, 5/6, 491
 Carretti, E., Poppi, S., Reich, W., et al. 2006, *MNRAS*, 367, 132
 Dineen, P., & Coles, P. 2005, *MNRAS*, 362, 403
 Efstathiou, G., & Bond, J. R. 1999, *MNRAS*, 304, 75

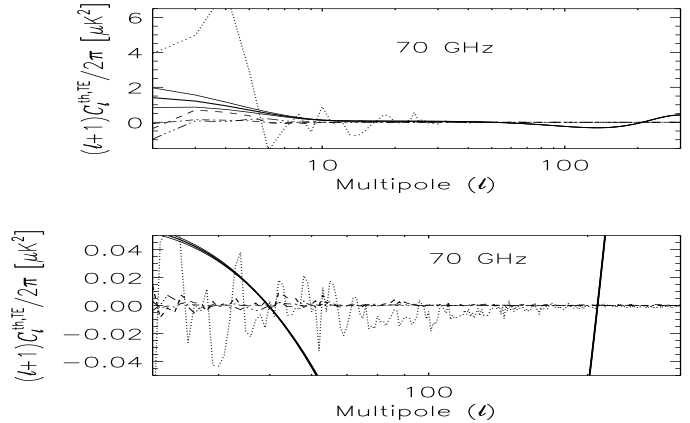


Fig. 5. Comparison between the TE modes of the CMB anisotropy and the Galactic diffuse emission. Solid lines: CMB TE mode with $T/S = 0.005$ (thick solid line) and corresponding cosmic variance (region between the thin solid lines), assuming all sky coverage and without binning in ℓ . Dots: extrapolated DRACO TE mode for a spectral index $\beta = -3$. Dashes (dot-dashes): as above, but masking the region at $|b_{gal}| \leq 5^\circ$ and adopting $\beta = -2.8$ ($\beta = -3$). Three dots-dashes: as above, but excluding the region at $|b_{gal}| \leq 20^\circ$ ($\beta = -2.8$). Top and bottom panels are identical, but with a different choice of the multipole and power range, for a better view of the results.

- Egger, R. J., & Aschenbach, B. 1995, *A&A*, 294, L25
 Ginzburg, V. L., & Syrovatskii, S. I. 1965, *ARA&A*, 3, 297
 Górski, K. M., Hivon, E., Banday, A. J. et al. 2005, *ApJ*, 622, 759
 Haslam, C. G. T. 1974, *A&AS*, 15, 333
 Johnston-Hollitt, M., Hollitt, C. P., & Ekers, R. D. 2004, in *The Magnetized Interstellar Medium*, ed. B. Uyaniker et al. (Copernicus GmbH), 13
 Kamionkowski, M., Kosowsky, A., & Stebbins, A. 1997, *Phys. Rev. D*, 55, 7368
 Knox, L., & Turner, M. S. 1994, *Phys. Rev. Lett.*, 73, 3347
 Kosowsky, A. 1999, *NewAR*, 43, 157
 Kogut, A. 2003, *NewAR*, 47, 977
 La Porta, L., & Burigana, C. 2006, *A&A*, accepted, astro-ph/0601371
 La Porta, L., Reich, P., Burigana, C., & Reich, W. 2005, *MPIfR-Memo*, 1
 Manchester, R. N., Han, J. L., Qiao, G. J. 1998, *MNRAS*, 295, 280
 Mesa, D., Baccigalupi, C., De Zotti, G. et al. 2002, *A&A*, 396, 463
 Page, L., Hinshaw, G., Komatsu, E. et al. 2006, *ApJ*, submitted, astro-ph/0603450
 Peebles, P. J. E. 1993, *Principles of Physical Cosmology*, Princeton University Press
 Peiris, H. V., Komatsu, E., Verde, L. et al. 2003, *ApJS*, 148, 213
 Prandoni, I., Gregorini, L., Parma, P. et al. 2001, *A&A*, 365, 392
 Reich, P., & Reich, W. 1986, *A&AS*, 63, 205
 Reich, W. 1982, *A&AS*, 48, 219
 Seljak, U., & Zaldarriaga, M. 1997, *Phys. Rev. Lett.*, 78, 2054
 Sokoloff, D. D., Bykov, A. A., Shukurov, A. et al. 1998, *MNRAS*, 299, 1985
 Spergel, D. N., Bean, R., Dore, O. et al. 2006, *ApJ*, submitted, astro-ph/0603449
 Toffolatti, L., Argüeso Gómez, F., De Zotti, G. et al. 1998, *MNRAS*, 297, 117
 Tucci, M., Martínez-González, E., Toffolatti, L. et al. 2004, *MNRAS*, 349, 1267

Wolleben, M. 2005, PhD Thesis, Bonn University, Germany

Wolleben, M., Landecker, T. L., Reich, W., & Wielebinski, R. 2006,
A&A, 448, 411

Zaldarriaga, M., & Seljak, U. 1998, Phys. Rev. D, 58, 3003

Zaldarriaga, M. 2001, Phys. Rev. D, 64, 15